SCIREA Journal of Mechanical Engineering

http://www.scirea.org/journal/Mechanical

January 1, 2023

Volume 4, Issue 1, February 2023

http://dx.doi.org/10.54647/mechanical46094

Electrification of a Retractor Consisting of Flexible Structure and Development of Six-D.o.F Surgical Assist Arm with Unactuated Joints

Toshihiro Yukawa[1,*], Kazushi Nakamura[1], Hiroki Satoh[1], Youichi Takeda[2], Yoshiaki Oshida[2], Jun Sasaki[3]

[1]Dept. of Mech. Eng., Faculty of Eng., Iwate University, 4-3-5, Ueda, Morioka, Iwate, 020-8551, Japan

[2]Division of Technical Support, Iwate University, 4-3-5, Ueda, Morioka, Iwate, 020-8551, Japan

[3]Iwate Medical University, 1-1-1 Idaidori, Yahaba-cho, Shiwa-gun, Iwate Prefecture 028-3694, Japan

*Corresponding author: yukawat@iwate-u.ac.jp

Abstract

In this paper, we describe a new type of a flexible retractor (universal fixator) and an assist arm with surgical instrument developed as substitutes for an abdominal retractor for use during surgery. The new assist arm as the retractor with surgical instrument can increase the efficiency of retraction function during surgery. As for the conventional flexible retractor, the amount of rotation of the knob required for fixing and loosening was large, and it took time to operate. To overcome this problem, we install a motor to the retractor and perform a torque control. On the other hand, our developed assistance mechanism has a six-D.o.F as high controllability at the tip of the mechanism. Also, the whole mechanism of the assist arm consists of a serial three-link

with three joints whose each joint is composed of a differential gear mechanism. The assist arm is able to maintain situation of the relevant body part of a person on the operating table while maintaining own posture.

Keywords: *retractor, flexible retractor, assist arm, surgical arm, fixation device, six-D.o.F manipulator, motor, differential gear mechanism, friction brake, brake pad, manipulability*

1. Introduction

We develop a new type of assistant surgical arm which has a six-D.o.F mechanism for with high controllability for use during surgery. The mechanism consists of a serial three-link manipulator whose each joint is composed of a differential gear mechanism. The instrument needs to maintain the shape of the relevant body part while maintaining own posture during surgery. The new instrument can increase the efficiency of surgical procedure during surgery.

In recent years, many researchers have developed robotic surgery and surgical instruments. Z. Li et al have derived the direct kinematics and resolved the inverse kinematics of the Raven IV surgical robot system [1]. The Area-Circumference ratio was used to evaluate the geometric properties of the common workspace of the four Raven IV arms. W. Wei et al have presented a new hybrid robotic system being developed for surgical procedures associated with hollow suspended organs. They have examined in ophthalmic surgery where the eyeball is a partially constrained hollow suspended organ. Dexterity improvements in manipulation and operation of the eyeball were quantified while using the proposed robot compared to traditional tools [2]. K. Kishi et al. have developed a dual-armed slave manipulator with magnetic resonance compatibility, spatial non-interference, and interchangeable surgical tools to support diagnosis and treatment, and the dual-armed master device to manipulate it. [3]. K. Sugiyama et al. have developed a remote-controlled surgical assistance robot. In animal puncture experiment, the operation of the robot was based on joint control. As a surgeon orders for a change in the direction of the needle, the tip of the needle moves, and the tip of the needle the remote control compensates the error while maintaining a high operation [4]. Z. Long et al. have developed a real-time arthroscopic system utilizing an endoscopic camera and optical fiber in order to navigate a normal vector for a reconstructed knee joint surface. A specific navigation approach suitable for use in a rendered surface was presented [5]. K. Takikawa et al. have developed a pneumatically-driven forceps manipulator for a master-

slave-type surgical robot. The proposed manipulator had two flexible joints, one for the bending joint at the tip and the other for transmitting a bending force from the actuators to the wires of the forceps. The manipulator has two-D.o.F of bending driven by two pneumatic cylinders and a gripper driven by the cylinder [6]. Y. Fujihira et al have developed a force feedback manipulator system for use in neurosurgery. The system consists of a multi degree of freedom manipulator with a force detecting gripper and a device capable of using force feedback to display kinesthetic sense. The structure consisting of parallel thin plates in the gripper of the manipulator can detect a gripping force and a pulling force which can be used to grip and pull tumors [7]. As a simple surgical instrument, a needle holder is one of surgical instruments is used by surgeons to hold a surgical suture and similar to a hemostat, for closing wounds during suturing in surgery. As a robot with the needle holder, the DEX robot has been designed to cut and dissect for a precise, and safe minimal invasive surgery while reducing surgeon discomfort and fatigue [8]. M. Donnici et al. have developed an image guided robotic system for needle positioning procedures using a CT scanner in order to aid the surgeon in inserting a needle into a tissue, and the terminal element for calibrating the end-effector [9]. H. M. Chien discussed that major difficulty and time consuming part of laparoscopy is suturing, and concluded that a new suture-friendly tool reduces the need for the hand-eye co-ordination and finding the thread [10].

In open abdominal surgery, supporting staffs have to hold the opening in the skin or internal organ of patient undergoing surgery for a long time. An appropriate retractor is able to maintain the shape of the relevant body part while maintaining own posture during surgery. For previous proposed retractor, or surgical instruments, some developed devices were driven by gas pressure, and it needed additional peripheral device [11]. T. Ranzani et al. have presented the concept design of a modular soft manipulator for minimally invasive surgery. Also, they have combined flexible fluidic actuators in order to obtain multidirectional bending and elongation with a variable stiffness mechanism based on granular jamming. Each module consists of a silicone matrix with pneumatic chambers for 3-D motion, and one central channel for the integration of granular-jamming-based stiffening mechanism [12]. F. Leong et al. have reviewed the implementation of magnetic based approaches in surgical instruments for abdominal surgeries. The evolution of surgical applications to the current popular approaches of MIS, LESS and NOTES integrated with the use of magnetic actuation emphasizes the benefits of magnetic systems in the field of abdominal surgery. Therefore, the concept of magnetic based techniques in robotic surgery demonstrates great potentials for

surgical innovations that could replace conventional abdominal surgery, elevating the surgical robotics field to the next technological level [13]. T. Watanabe et al. have presented a force-visually-observable silicone retractor, which is an extension of a previously developed system that had the same functions of retracting, suction, and force sensing. These features provided not only high usability by reducing the number of tool changes, but also a safe choice of retracting by visualized force information. Suction was achieved by attaching the retractor to a suction pipe. The retractor has a deformable sensing component including a hole filled with a liquid [14]. A. Razjigaev et al. have developed a patient-specific low-cost 3D printable snake-like manipulator, and it was teleoperated. This snake-like tool was modelled to be parametric for patient-specific interventions in fiber-optic knee arthroscopy requiring an inverse kinematic controller that can steer the position and orientation of the tip. The teleoperation system successfully allowed the user to steer the tip at different positions and orientations in a test teleoperation task [15]. K-Y Kim et al. have proposed a surgical manipulator with workspace conversion ability for performing both an MIS procedure and an open surgical procedure. They have proposed the surgical manipulator with distal rolling joint which is implemented with two spiral wire ropes. Also, an attachment and detachment of the surgical tool unit without other assistance were carried out using a developed tool loader [16]. C. D. Natali et al. have developed the system which enhances both the workspace of operation and triangulation without the need for multiple abdominal incisions while interrupting the mechanical continuity of such system by having surgical instruments and laparoscopic camera magnetically coupled across the abdominal wall greatly. Their continuum robots have ability to provide a large amount of mechanical power to accomplish surgical tasks [17].

2. Improvement of Conventional Retractor

2. 1. Reduction of Operating Force of Conventional Retractor

2. 1. 1. Calculation of Operating Force

A retractor consisting of flexible joints for fixing brain with spatula made by Mizuho Corporation is shown in Figure 1. The retractor consisting of flexible parts is made of stainless steel, and it has a structure in which multiple ball joints and cylinders are connected one after the other. By pulling stainless steel wire passing through the center of cross section surface of the ball joints and cylinders, the force is being applied between the cylinder and the ball at each joint of the body, the posture of the whole body can be fixed by frictional force

generated at each contact point between them. Although the advantage of the retractor is that it can be fixed even in any position, or posture due to its flexible structure, the knob for fixing must be turned manually in the original product, and a very large force was required. In order to improve the problem, we first obtain the torque for turning the knob.

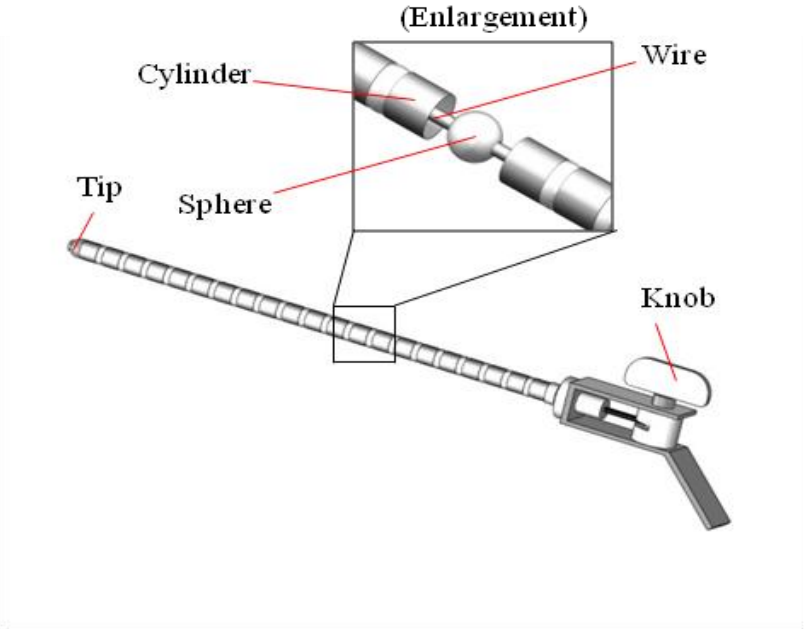

Figure 1. A retractor consisting of flexible structure

The external tensile force P N applied to the wire is calculated as follows. Let ΔL m be the elongation of the wire, E GPa be Young's modulus, d m be the diameter of the wire, $A(=\pi d^2/4)$ m^2 be the cross-sectional area of the wire, and L m be the length of the wire. According to Hooke's law, it is expressed as follows:

$$P = \frac{\Delta L E A}{L} \quad , \tag{1}$$

where E = 200 GPa, d = 0.0025 m, A = 4.909×10^{-6} m^2 and L = 0.370 m.

Therefore, P N is specifically calculated as:

$$P = 2.653 \times 10^6 \times \Delta L \, . \tag{2}$$

Setting the distance from the rotation center axis of the knob to the wire fixing point as r = 0.015 m, the torque T_0 Nm required to turn the fixing knob can be calculated as follows:

$$T_o = P r = 0.015 \, P$$

$$= 39{,}795 \, \Delta L \, . \tag{3}$$

2. 1. 2. Reduction of Operating Force

The conventional flexible retractor is required a large force to release the fixing of each joint, originally.

Here, in order to reduce the input torque for turning the knob, we design a retractor using a reduction gear mechanism incorporating a screw gear mechanism and a worm wheel mechanism. Figure 2 shows the appearance of the improved part in the retractor. Figure 3 shows the inside of the improved mechanism as shown in Figure 2. As shown in Figure 2 and Figure 3, the screw gear mechanism is installed on the rotation axis of the fixing knob, and the

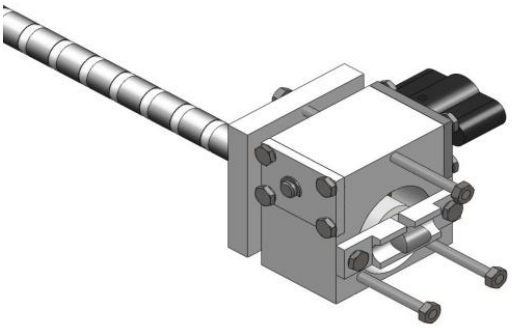

Figure 2. The peripheral part of the improved fixing knob

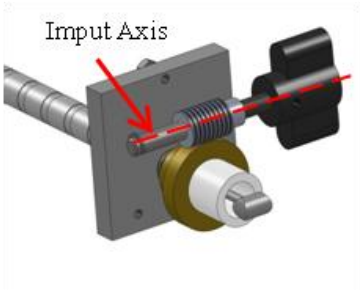

Figure 3. The structure of the internal side

worm wheel is set between the parts for fixing joints and the screw gear. Defining the number of threads of the worm gear to be Z_1 and the number of teeth of the wheel to be Z_2, the reduction ratio n from the rotation of the knob to the one of worm wheel can be given by the following relationship:

$$n = \frac{Z_2}{Z_1}. \tag{4}$$

Setting the transmission efficiency of the worm gear as η, the relationship between the input torque T Nm and the output torque T_H Nm can be expressed by the following equation:

$$T_H = \eta\, n\, T\ . \tag{5}$$

Next, we obtain the relationship between the torque applied to the worm wheel and the force (screw thrust) Q that pulls the internal wire passing through inside the arm. Define the lead angle α rad of the screw gear, the apex angle β rad, the friction angle θ rad, and the effective diameter D m. Then, the thrust force Q N of the screw gear becomes as follows:

$$Q = \frac{2\ T_{\mathrm{H}} \cos\beta}{D \tan(\alpha+\theta)}\ , \tag{6}$$

where the friction angle θ rad can be calculated using the dynamic friction coefficient μ as follows:

$$\theta = \tan^{-1}\mu\ . \tag{7}$$

The external tensile force P in (2) and the screw thrust Q in (6) satisfy the following relationship as:

$$P = Q\ . \tag{8}$$

From (2), (5), (6), and (7), the input torque T Nm is given by:

$$T = \frac{D \tan(\alpha+\tan^{-1}\mu)}{2\,n\,\eta\,\cos\beta}\ P\ , \tag{9}$$

where D = 0.010 m, α = 1°57′ (= 13π / 1200 rad), β = π/6 rad, μ = 0.21, n = 50 and η = 0.4.

Therefore, the input torque T Nm becomes:

$$T = 188.25\ \Delta L\ . \tag{10}$$

From (3) and (9), the following equation:

$$T = 0.00473\ T_0 \tag{11}$$

can be derived.

Theoretically, the required torque after improvement of the flexible retractor becomes 0.473 % of the required torque before one.

2. 1. 3. Experiment of Force/Torque Transmission

Here, we measure the input torque T required to maintain the posture of retractor indefinitely as the posture of retractor is being fixed. A specification of the payload of the flexible retractor is defined as the retractor can have a function for holding the posture with a weight of 49.0 N (= 5.0 kgf) attached to the tip of the retractor in a horizontal posture. As a result, it was confirmed when the elongation of the wire was ΔL = 6.5 mm, the retractor was able to fix each joint while maintaining a horizontal posture in experiment. As an operator applies a load to the hook attached to the tip of the knob gradually measures the load F at the moment when the knob starts to rotate. The load torque can be calculated from the measured value of the load F and the distance r from the center axis of the knob to the load point, as shown in Figure 4. From F =5.0 kgf (= 49.0 N) and r = 0.020 m, T Nm is given by:

$$T = F\,r = 0.980\ . \tag{12}$$

From (9), the theoretical value of the torque T becomes T = 1.224 Nm, and it can be seen that there is a difference of about 20 % between the measured value derived in (12) and the theoretical one. This result is due to factors such as increase in necessary thrust by means of the friction generated at the sliding part. As several people tried it as trial subjects, it was easy to turn and their hands did not get tired easily. However, the amount of rotation of the knob required for fixing and loosening was large, and it took time to operate. In order to deal with this problem, we try to install a motor to the retractor and perform a torque control.

2. 2. Retractor with Automatic Control

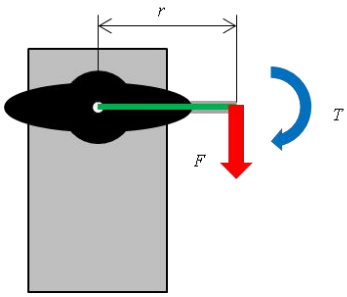

Figure 4. Torque measurement experiment

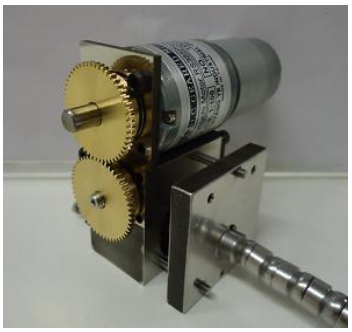

Figure 5. The improved flexible retractor with a motor

2. 2. 1. Design of the Control System

The DC motor installed on the retractor is RS-385PH-17120 (manufactured by Mabuchi Motor, the reduction ratio of the geared motor is 1/100). Figure 5 shows the mechanism that transmits the output torque of the motor to the input axis of the knob shaft, as shown in Figure 3. Setting the output torque of the motor as the parameters T_{M} Nm, the efficiency of the geared motor as η_{r} the reduction ratio of the geared motor as n_{r}, the transmission efficiency of the spur gear as η_{g} and the reduction ratio of the spur gear as n_{g}, the output torque T is given by:

$$T = \eta_{\mathrm{r}}\,\eta_{\mathrm{g}}\,n_{\mathrm{r}}\,n_{\mathrm{g}}T_{\mathrm{M}}\ . \tag{13}$$

Therefore, from (11), the output torque generated by the motor required to fix the retractor posture becomes:

$$T_{\mathrm{M}} = \frac{T}{\eta_{\mathrm{r}}\,\eta_{\mathrm{g}}\,n_{\mathrm{r}}\,n_{\mathrm{g}}} \tag{14}$$

Substituting n_r = 100, η_r = 0.60, n_g = 1, η_g = 0.98 and T = 0.980 Nm derived from (11) into (14),

$$T_M = 0.0167 \tag{15}$$

can be obtained. From torque-current characteristics of the motor shown in Figure 6, the current flow as each joint of the retractor is fixed is about 0.7 [A], the current value was used for motor control.

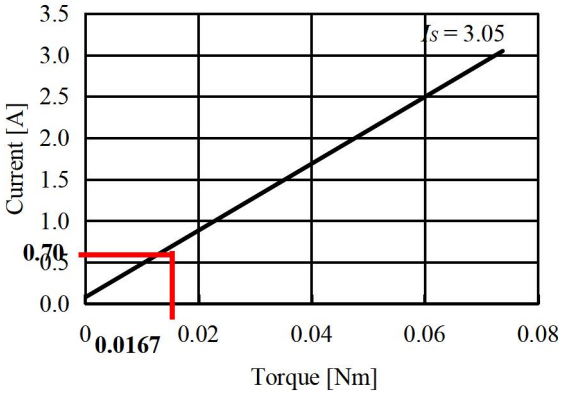

Figure 6. Torque - current curve

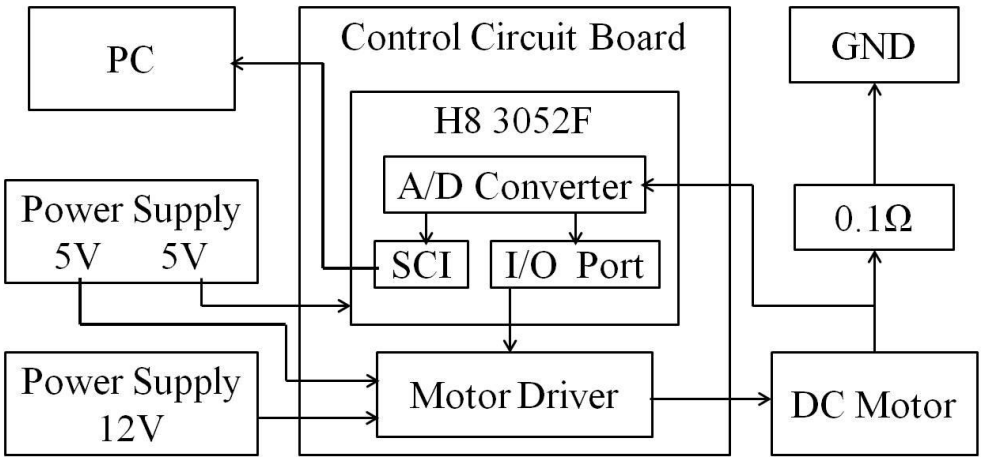

Figure 7. Control system configuration of DC motor

2. 2. 2. Motor Control Circuit

In order to control the DC motor, H8 3052F microcomputer (manufactured by Renesas Technology), operational amplifier LM358N (manufactured by HTC) and motor driver STK681-210-E (manufactured by SANYO) are used. The system configuration diagram of

the DC motor is shown in Figure 7. As a flow of fixation/release control for the retractor, the wire is wound and all joints are fixed when push switch 1 on the control board is pushed as the motor rotates in forward direction, while the wire is loosen and all joints are unlocked when push switch 2 is pushed as the motor rotates in reverse direction. The motor stops when either forward/reverse button switch is turned on, or off. As shown in Figure 8, a resistor of 0.1 Ω is provided as a shunt resistor on the negative side of the DC motor, and the voltage across the resistor is amplified by an operational amplifier. The voltage value is inputted to the microcomputer by way of the A/D port in the H8 microcomputer, and the current consumed by the motor is calculated using C language software installed in the computer. A brake control for the motor is performed just as the current value exceeds 0.7 [A]. The maximum current of the motor driver is Is = 3.05 A. It is possible to send data to a PC using the serial communication interface (SCI function) in the H8 microcomputer.

2. 2. 3. Torque Control Experiment

Setting the wire elongation ΔL = 3.0 mm as the initial position, an operator keeps pressing switch 1 in order to control the rotation of the motor. We examine the elongation of the wire just as the motor is stopped by the control program.

At the same time, the data of the current value to the personal computer is sent every 0.5 s through the SCI function in the microcomputer, graphs of the relationship between the current and time is drawn on the monitor. In the experiment, the elongation of the wire immediately when the motor stopped was ΔL = 6.4 mm. Figure 9 shows the time response of the current value at that time.

3. Development of Six-D.o.F Retractor

3. 1. Surgical Manipulator with Differential Gear Mechanism

As one of surgical instrument, we develop an abdominal retractor which has six-D.o.F with

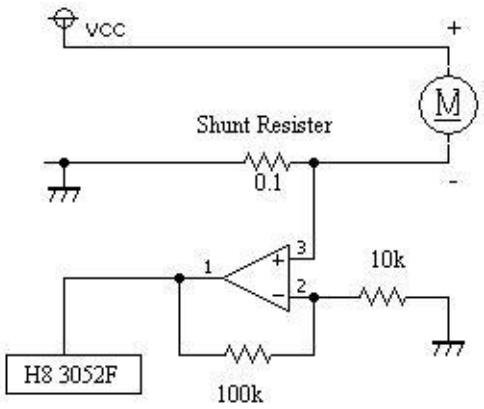

Figure 8. Current measurement circuit

high reliability. As design criteria for the retractor, the surgeon's area of the patient is set

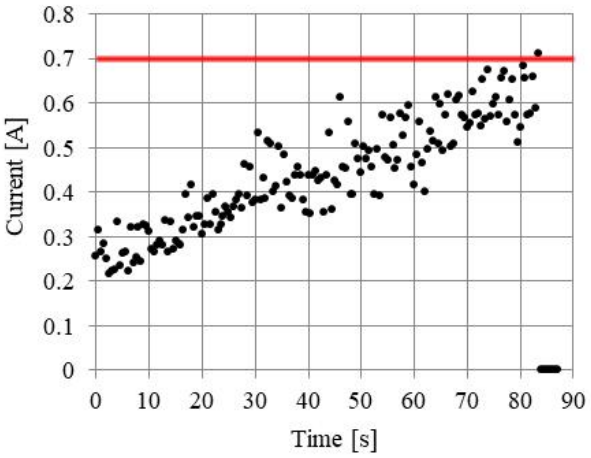

Figure 9. The time responses of current generating in the motor

as a larger area than the general tissue opening. To be specific, the range of movement of the tip of the fixing device is set within a rectangle of 200 mm as considering the length of each link. Structural design of a lever for operating a fixing device holding the tissue opening may require a high operability that a surgeon is able to operate the lever with one hand alone. The permissible operating angle of each joint is designed as $\pi/6$ rad due to its constraints on load, movable range and mechanical structure. Although the range of each joint angle might be comparatively small, the range in open abdominal surgery, or open chest surgery is enough to operate. Each joint with a differential gear mechanism can be driven simultaneously by operator's manual operation from the base side through a screw gear train. That is, the fixation of all joints can be controlled by operation by a surgeon's hands. The proposed retractor is shown in Figure 10. Each joint has two degrees of freedom because of a feature of differential

gear mechanism. Since the retractor has three joints, total degree of freedom of the tip becomes six degrees of freedom. Therefore, the tip of the retractor can be kept at an arbitrary position and posture. Each joint is being fixed in the case when the rubber wheel and the brake plate are being fixed. The rubber wheel continues to push the brake plate in case where anyone does not take the handle of the brake lever.

Figure 10. Six-D.o.F retractor

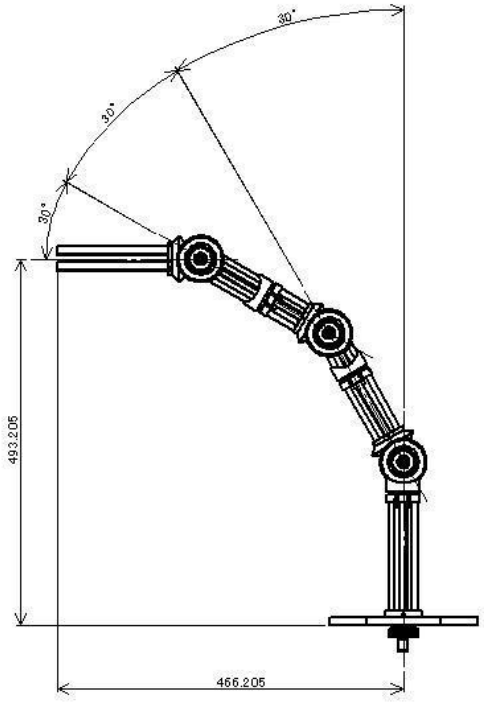

Figure 11. Range of movement of retractor

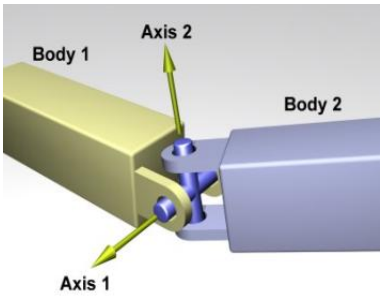

Figure 12. A universal joint

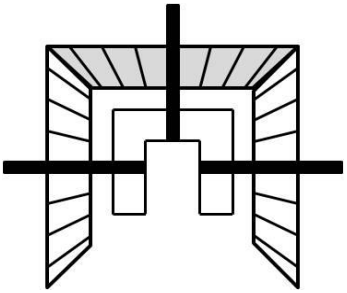

Figure 13. A differential gear mechanism

However, it is understood when moving the tip of the retractor between two points, there was a disadvantage that the trajectory of the tip and arbitrarily trajectory of each joint cannot be determined arbitrarily, and the workability of the retractor was low. Figure 11 shows appearance, size and range of movement of the retractor.

3. 2. Mechanism of the Six-D.o.F Retractor

Here, we explain a design of a device that can fix all joints by moving only one knob. It took time to fix the arm for the conventional retractors with multi-degree-of-freedom mechanism for fixation which has several brake knobs. In order to move the tip of the device freely, we design it with six degrees of freedom, and the number of links is set to four. A universal joint, as shown in Figure 12 installed in the retractor is used to transmit the power of the knob in order to fix each joint in its any posture. The joint part consists of a differential gear mechanism with bevel gears, as shown in Figure 13. The differential gear mechanism synthesizes motions of two or more gears into one motion, and outputs the motion. A mechanism combining three bevel gears is used, this time for the differential gear mechanism. By installing this joint in three stages, all the rotation of the trapezoidal screw gear shaft can be transmitted to each joint through a universal joint at the same time and all joints can be fixed. The universal joint has the characteristic that it does not affect the transmission of rotation even if the relative position or angle between two axes is changed. As the left and right gears rotate in the same direction, the entire joint bends around the axis of the left and right gears, whereas as these rotate in the opposite direction, only the upper gear rotates, as shown in Figure 13. As a means of fixing the rotation of the differential gear, a couple of rubber wheels which is attached to the left and right bevel gears by a slide mechanism using trapezoidal screw gears gradually approach the braking surfaces, which are fixed to the adjacent links, and are fixed by friction due to pressing force after the wheel contacts the braking surfaces. Stated slightly differently, the pull force generated by the rotation power of the screw maintains the entire posture of the retractor. As the rubber wheel is stuck with the brake plate by frictional force between them or deformation of the rubber, each joint becomes under a fixed situation. As turning the knob by hand in the opposite direction, the pressure generated between rubber wheel and the brake plate weakens. Then, each joint is released amd being free as the rubber wheel is separated from the brake plate. Approximate static friction coefficient between both materials of the rubber wheel and the brake plate was assumed to μ = 0.3-0.8. In order to enlarge the frictional force, we applied the rubber wheel with fat tire as the brake pads. Since allowable operating angle of each universal joint is limited within $\pm\pi/6$ rad structurally, we designed the movable range of the first and second turning angles of the joint to be $\pi/6$ rad. As a result in the operation experiment at the design and manufacturing stage, the trapezoidal screw gear is interfered with both the first and second rotary joints, then the position of the brake plate was moved by θ_2/π and $(\theta_2+\theta_4)/\pi$ mm,

respectively. As for the structure using a differential gear when the normal range of θ_2 and θ_4, which can be useful with mechanical limiter is set to $\pm \pi$ rad, then the brake plate moves by a maximum of 2.0 mm. The rubber wheel, which is used as the brake pad makes it possible to compensate for the maximum amount of motion and mechanical errors of the brake plate, which is faced against it, and fix all joints within the normal range of use. Thus, as the left and right gears are fixed, the joint is completely fixed, furthermore the retractor is fixed. As above mentioned, the advantage in operability of the retractor is that fixation and release of all joints can be performed simultaneously by using a knob installed on the base side.

3. 3. Solution Method of Forward Kinematics using Denavit-Hartenberg Method

Here, we obtain a simultaneous transformation matrix of the proposed retractor based on the Denavit-Hartenberg (DH) method, solve the forward kinematics and obtain the coordinates of the tip position. Set the coordinate system for each joint (i = 1 to 6) of the retractor, as shown in Figure 14. Table 1 shows the link parameters of the retractor. The link parameters are represented as follows; i) translation along the X_i - axis by $a_{i\text{-}1}$, ii) rotation by $\alpha_{i\text{-}1}$ around the $X_{i\text{-}1}$-axis, iii) translation along the Z_i-axis by d_i, and iv) rotation by θ_i along the Z_i-axis. From i) - iv), the homogeneous transformation matrix becomes:

$$ {}^{i\text{-}1}T_i = \begin{bmatrix} C_i & -S_i & 0 & a_{i\text{-}1} \\ C_\alpha S_i & C_\alpha C_i & -S_\alpha & -S_\alpha d_i \\ S_\alpha S_i & S_\alpha C_i & C_\alpha & -C_\alpha d_i \\ 0 & 0 & 0 & 1 \end{bmatrix}, \tag{16} $$

Table 1. Link parameters of the retractor

i	a_{i-1}	α_{i-1}	d_i	θ_i
1	0	0°	0	θ_1
2	0	-90°	L_2	θ_2
3	0	90°	0	θ_3
4	0	-90°	L_3	θ_4
5	0	90°	0	θ_5
6	0	-90°	0	θ_6
E	0	0°	L_4	0°

where each notation represents C_i = cos θ_i, S_i = sin θ_i, C_α = cos $\alpha_{i\text{-}1}$, and S_α = sin $\alpha_{i\text{-}1}$, respectively. For the global coordinate system Σ_R , the local coordinate system Σ_E representing the position and orientation of the tip of the retractor can be expressed using ${}^RT_E$ as:

$$ {}^RT_E = {}^RT_0\,{}^0T_1\,{}^1T_2\,{}^2T_3\,{}^3T_4\,{}^4T_5\,{}^5T_6\,{}^6T_E $$

$$\equiv \begin{bmatrix} R_{11} & R_{12} & R_{13} & p_X \\ R_{21} & R_{22} & R_{23} & p_Y \\ R_{31} & R_{32} & R_{33} & p_Z \\ 0 & 0 & 0 & 1 \end{bmatrix}, \tag{17}$$

where R_{11} to R_{33} represent the rotation matrices, and p_X, p_Y, and p_Z represent the X, Y and Z coordinates of the tip position as:

$$p_X = C_1[C_2\{-S_3(C_5L_4+L_3)-C_3C_4S_5L_4\}+S_2S_4S_5L_4]-S_1\{C_3(C_5L_4+L_3)-C_4S_3S_5L_4+L_2\} \tag{18}$$

$$p_Y = S_1[C_2\{-S_3(C_5L_4+L_3)-C_3C_4S_5L_4\}+ S_2S_4S_5L_4]+C_1\{C_3(C_5L_4+L_3)-C_4S_3S_5L_4+L_2\}+L_1 \tag{19}$$

$$p_Z = C_2S_4S_5L4-S_2\{-S_3(C_5L_4+L_3)-C_3C_4S_5L_4\} \ , \tag{20}$$

respectively.

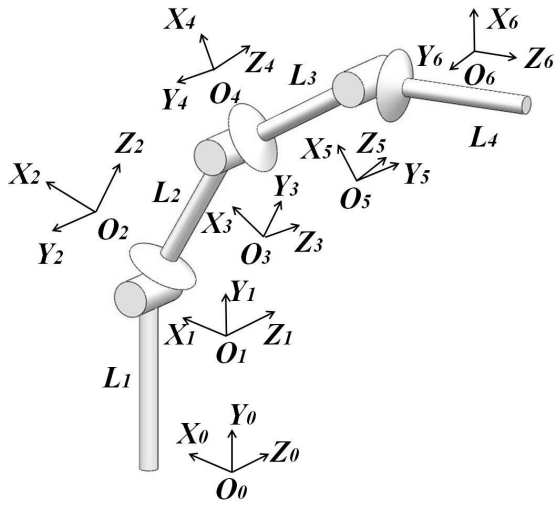

Figure 14. The coordinate system for each joint of retractor

3. 4. Relationship between Forces Acting on the Tip and Joint Torque

The Jacobian matrix $J(\theta)$ of the six-D.o.F retractor is expressed as:

$$\boldsymbol{J}(\boldsymbol{\theta}) = \begin{bmatrix} J_{11} & J_{12} & J_{13} & J_{14} & J_{15} & J_{16} \\ J_{21} & J_{22} & J_{23} & J_{24} & J_{25} & J_{26} \\ J_{31} & J_{32} & J_{33} & J_{34} & J_{35} & J_{36} \end{bmatrix}, \tag{21}$$

and the following mathematical relationship can be satisfied as:

$$\frac{d\boldsymbol{P}}{dt} = \boldsymbol{J}(\boldsymbol{\theta}) \frac{d\boldsymbol{\theta}}{dt} \ , \tag{22}$$

where $\boldsymbol{P} = [p_X, p_Y, p_Z]^T$ and $\boldsymbol{\theta} = [\theta_1, \theta_2, \theta_3, \theta_4, \theta_5, \theta_6]^T$.

Also, the relationship between torque τ and f is given by [2)]

$$\boldsymbol{\tau} = \boldsymbol{J}^T \boldsymbol{f} \ . \tag{23}$$

Using the upper equation, the force at the tip can be converted into each joint torque.

3. 5. Calculation of Maximum Static Friction Torque Generated Using Brake Mechanism

Here, we calculate the static torque to support the posture of the retractor using the brake mechanism. The structure of a brake mechanism and a knob consisting of several parts is shown in Figure 15. A conduction mechanism consisting of screw gear and nut mechanism passing inside the arm are used to maintain its posture.

The load P N as the rubber is deformed by Δb m due to the brake plate is derived, first. Setting the Young's modulus of rubber as E Pa, the thickness of the rubber wheel as b m, and the contact area between the brake plate and the rubber wheel as A m^2, the formula which can be obtained from Hooke's law becomes:

$$P = \frac{\Delta b\, E\, A}{b}. \tag{24}$$

Setting the coefficient of static friction as μ, and the maximum static torque as T, the torque T when the radius of the rubber wheel is r mm becomes:

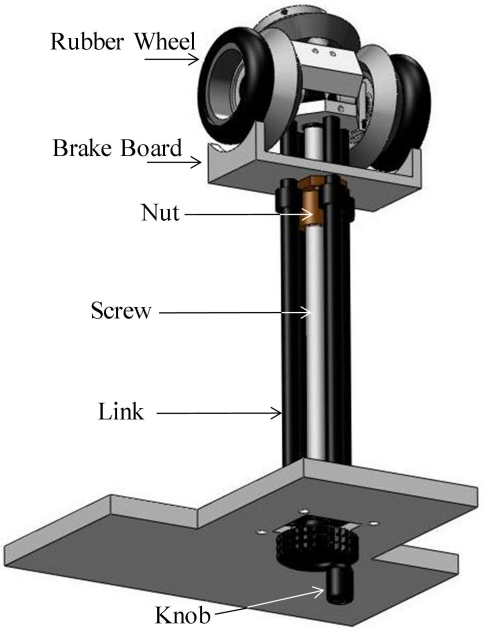

Figure 15. A brake mechanism and a knob

$$T = \mu P (r - \delta) = \frac{\mu \Delta b (r - \Delta b) EA}{b}. \tag{25}$$

The rotation angle of the differential gear is changed directly by the rotation angle of the knob. Also the magnitude of the load and torque at the tip of the fixing device depends on the amount of the rotation angle of the knob. As the screw gear is rotated inversely by inverse rotation of the knob, the rubber wheel separates from the brake plate and each retractor becomes in the state of a free joint arm.

3. 6. Experiment

Figure 16 shows the appearance of the retractor. The same three joints are used for each joint installed in the proposed retractor. Figure 16(a) shows the front view of the retractor, and Figure 16(b) shows the side view of it. The conduction mechanism transmits the power to each joint in any posture, and fixes all the joints simultaneously. The movable range is sufficient to the operation, and also the controllability and operatively can be compensated. First, we confirm whether each joint can be fixed, or not in the posture of the retractor with the condition of first joint angle $\theta_2 = \pi$ rad, and the second one $\theta_4 = \pi$ rad. That is, a load was applied to the tip position in the X direction while standing the retractor upright. Figure 17 shows the situation in torque measurement experiment. Since the largest torque is generated at the first joint, the torque generating at the moment when the first joint begins to move is taken

(a) Front view **(b) Side view**

Figure 16. Appearance of the retractor

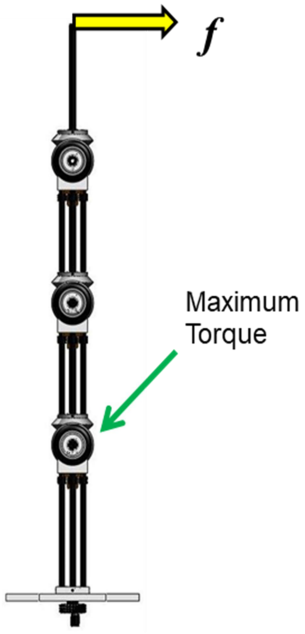

Figure 17. Torque measurement experiment

as the maximum static torque of the entire manipulator. As the manual brake was applied, the displacement δ of the rubber was 2.0 mm. In the experiment, it was actually confirmed that each joint was fixed within the range of normal use. Substituting the parameters μ = 0.75, r = 0.029 m, E = 14.2 MPa, A = 225×10^{-6} m^2, b = 6.0 mm into (25), the theoretical value T becomes T = 21.566 Nm. The load at the moment when the first joint started to move was 3.3 kgf (= 32.34 N) gives the maximum static torque $T_f = 3.3 \times 9.8 \times 0.6 = 19.40$ Nm under the actual length condition of $L_2 = L_3 = L_4$ = 0.20 m. About the comparison of the load there was a difference of 2.162 Nm between the theoretical value and the experimental one. The reason for this difference was caused by the rubber of the brake material deteriorated and hardened, and furthermore, results in a decrease in Young's modulus.

4. Conclusions

In this paper, we have motorized for the conventional universal spatula fixator in order to improve usability and evaluated it. Also, we have developed a retractor with a linkage mechanism for holding posture itself and the opening in the skin or internal organ of patient undergoing surgery for a long time. A six-D.o.F retractor equipped with a simultaneous fixation mechanism for all joints in order to reduce the operating force of the fixation knob for ease of use was developed and evaluated. Each joint consisting of rubber wheel and brake plate were introduced to the retractor in order to improve fixing method in order to enhance the holding force by friction in the joint. The proposed fixation device is based on a six-D.o.F serial link and joints. As each link is composed of metal flames, reduction of the weight of the apparatus was realized. Both fixation devices we dealt with was accomplished by brake mechanism at each joint. The brake mechanism was able to fix each joint simultaneously, and an articulated mechanism was able to move a restricted working space horizontally and vertically on an operating table. As a result, the proposed instruments increased the efficiency of surgery.

References

[1] Li, Z., Glozman, D., Milutinovic, D. and Rosen, J., Maximizing Dexterous Workspace and Optimal Port Placement of a Multi-Arm Surgical Robot, 2011 IEEE Int. Conf. on Robotics and Automation, 3394-3399, May. 9-13, 2011.

[2] Wei, W., Goldman, R. E., Fine, H. F., Chang, S. and Simaan, N., Performance Evaluation for Multi-arm Manipulation of Hollow Suspended Organs, IEEE Trans., Robotics, Vol. 25, No. 1, 147-157, Feb., 2009.

[3] Kishi, K., Kan, K., Fujie, M. G., Sudo, K., Takamoto, S. and Dohi, T., Dual-Armed Surgical Master-Slave Manipulator System with MR Compatibility, J. of Robotics and Mechatronics (JRM), Vol.17, No.3, 285-292, 2005.

[4] Sugiyama, K., Matsuno, T., Kamegawa, T., Hiraki, T., Nakaya, H., Nakamura, M., Yanou, A. and Minami, M., Needle Tip Position Accuracy Evaluation Experiment for Puncture Robot in Remote Center Control, J. of Robotics and Mechatronics (JRM), Vol. 28, No. 6, 911-920, 2016.

[5] Long, Z., Nagamune, K., Kuroda, R. and Kurosaka, M., Real-Time 3D Visualization and Navigation Using Fiber-Based Endoscopic System for Arthroscopic Surgery, JACIII Vol.20, No. 5, 735-742, 2016.

[6] Takikawa, K., Miyazaki, R., Kanno, T., Endo, G. and Kawashima, K., Pneumatically Driven Multi-DOF Surgical Forceps Manipulator with a Bending Joint Mechanism Using Elastic Bodies, J. of Robotics and Mechatronics (JRM), Vol. 28, No. 4, 559-567, 2016.

[7] Fujihira, Y., Hanyu, T., Kanada, Y., Yoneyama, T., Watanabe, T. and Kagawa, H., Gripping Force Feedback System for Neurosurgery, Int. J. of Automation Technology (IJAT), Vol. 8, No. 1, 83-94, 2014.

[8] DEX, Agile Robot, http://www.dexteritesurgical.com.

[9] Donnici, M., Lupinacci, G., Nudo, P., Perrelli, M. and Danieli, G., Using Navi-Robot and a CT Scanner to Guide Biopsy Needles, Int. J. of Automation Technology (IJAT), Vol. 11, No.3, 450-458, 2017.

[10] Chien, H. M., Novel Laparoscopic Needle Holder, MATEC Web of Conferences, 2016 8th Int. Conf. on Computer and Automation Engineering (ICCAE 2016), Vol. 56, 08002, 2016.

[11] Mitaka Kohki Co., Ltd., Medical Equipment/instrument, http://www.mitakakohki.co.jp/english/medical/ .

[12] Ranzani, T., Cianchetti, M., Gerboni, G., Falco, I. D. and Menciassi, A., A Soft Modular Manipulator for Minimally Invasive Surgery: Design and Characterization of a Single Module, IEEE Trans. on Robotics, Vol. 32, Issue 1, 187 - 200, Feb., 2016.

[13] Leong, F., Garbin, N., Natali, C. D., Mohammadi, A., Thiruchelvam, D., Oetomo, D. and Valdastri, P., Magnetic Surgical Instruments for Robotic Abdominal Surgery, IEEE Reviews in Biomedical Engineering, 9:1-1, Feb. 2016.

[14] Watanabe, T., Koyama, T., Yoneyama, T. and Nakada, M., A Force-Visualized Silicone Retractor Attachable to Surgical Suction Pipes, Journals Sensors, Vol. 17, Issue 4, 17(4), 773, 2017.

[15] Razjigaev, A., Pandey, A. K., Howard, D., Roberts, J. and Wu, L., SnakeRaven: Teleoperation of a 3D Printed Snake-like Manipulator Integrated to the RAVEN II Surgical Robot, Project: Continuum Robots for Minimally Invasive Surgery, https://www.researchgate.net/publication/353915273, Sept. 2021.

[16] Kim, K. Y., Song, H. S, Suh J. W. and Lee, J. J., A Novel Surgical Manipulator with Workspace-Conversion Ability for Telesurgery, IEEE/ASME Trans. on Mech., Vol. 18, No. 1, 200-211, 2013.

[17] Natali, C. D., Mohammadi, A., Oetomo, D., Valdastri, P., Surgical Robotic Manipulator Based on Local Magnetic Actuation, ASME, J. Medical Devices, Vol. 9, 030936-1, Sept. 2015.